Journal of Experimental and Theoretical Physics, Vol. 90, No. 6, 2000, pp. 1093–1104.
Translated from Zhurnal Éksperimental'noĭ i Teoreticheskoĭ Fiziki, Vol. 117, No. 6, 2000, pp. 1255–1269.

SOLIDS
Electronic Properties

Interwell Excitons in GaAs/AlGaAs Double Quantum Wells and Their Collective Properties

A. V. Larionov*, V. B. Timofeev*, **, J. Hvam*, and K. Soerensen*****

**Institute of Solid State Physics, Russian Academy of Sciences, Chernogolovka, Moscow oblast, 142432, Russia*
***e-mail: timofeev@issp.ac.ru*
****Microelectronic Centre, DK 2800 Lyngby, Denmark*

Received February 17, 2000

Abstract—Luminescence spectra of interwell excitons in GaAs/AlGaAs double quantum wells with electric-field-tilted bands (*n–i–n*) structures were studied. In these structures the electron and the hole in the interwell exciton are spatially separated between neighboring quantum wells by a narrow AlAs barrier. Under resonant excitation by circularly polarized light the luminescence line of the interwell excitons exhibited appreciable narrowing as their concentration increased and the degree of circular polarization of the photoluminescence increased substantially. Under resonant excitation by linearly polarized light the alignment of the interwell excitons increased as a threshold process with increasing optical pumping. By analyzing time-resolved spectra and the kinetics of the photoluminescence intensity under pulsed excitation it was established that under these conditions the rate of radiative recombination increases substantially. The observed effect occurs at below-critical temperatures and is interpreted in terms of the collective behavior of the interwell excitons. Studies of the luminescence spectra in a magnetic field showed that the collective exciton phase is dielectric and in this phase the interwell excitons retain their individual properties. © *2000 MAIK "Nauka/Interperiodica".*

1. INTRODUCTION

Quasi-two-dimensional systems, double quantum wells, and superlattices are attracting interest in particular because of the fundamental possibility of spatially separating photoexcited electron and hole carriers between neighboring quantum wells [1–15]. In double quantum wells with an applied electric field which tilts the bands, excitons can be excited whose electron and hole are situated in different quantum wells separated by a barrier transparent to tunneling. These excitons are called spatially indirect (I) or interwell excitons in contrast to the direct intrawell excitons (D) where the electron and the hole in the exciton are located in the same quantum wells. Interwell excitons are long-lived compared with intrawell excitons so that they can easily build up, and a gas consisting of these excitons can be cooled to fairly low temperatures. As a result of destroyed inversion symmetry, interwell excitons have a dipole moment even in the ground state. The theory predicts various possible scenarios for collective behavior in a fairly dense system of spatially separated electrons and holes [1, 9–14]. It was shown in [14] that despite the dipole–dipole repulsion of interwell excitons, for certain critical parameters, i.e., the dipole moment of the interwell excitons, their density, and temperature, the stable state in the *e–h* system may be the liquid dielectric phase of these excitons. In an earlier study [11] it was noted that the condensed dielectric exciton phase can only occur in the presence of lateral confinement (random or artificially produced) in the quantum-well plane. Under these confinement conditions and the associated external compression, it is easier for excitons to build up to high critical densities sufficient for the appearance of collective exciton interaction effects.

It should be borne in mind that in real semiconducting-heterostructure tunnel-coupled quantum systems there is always a random potential as a result of various structural defects, i.e., residual impurities, charged and neutral, fluctuations of the barrier width and the widths of the quantum wells themselves, and so on. These fluctuations create a random potential relief in the quantum-well planes so that photoexcited electrons and holes spatially separated between neighboring wells, and also interwell excitons are highly localized at these fluctuations at fairly low temperatures. This strong localization effect in coupled quantum systems is manifest in particular in lateral thermoactivated carrier tunneling and is observed in experiments to study spectral narrowing of the luminescence line with increasing temperature, which corresponds to interwell radiative recombination [7].

In the present study we investigate the photoluminescence of interwell excitons in double quantum wells with a barrier containing four AlAs monolayers separating the quantum wells. With such narrow barriers the interwell excitons are fairly strongly coupled. Under these conditions the interwell excitons are localized at lateral fluctuations of the random potential without any significant changes in their internal structure if the linear scales of the fluctuations are $l > a_B$ (Bohr radius of an exciton $a_B \leq 100$ Å) and the fluctuation amplitudes are $\Delta > kT$. We know that in structures with narrow AlAs barriers the fluctuations of the barrier width are

large-scale and consequently the corresponding fluctuations of the lateral potential relief will also be large-scale. It is naturally predicted that at fairly low temperatures interwell excitons will be located in these large-scale random lateral potential wells. It is interesting to know whether a system of interwell excitons under conditions of such random lateral confinement will demonstrate critical behavior with increasing density and at fairly low temperatures. In the present paper we attempt to answer these questions.

The paper is constructed as follows. After describing the double-quantum-well heterostructures being studied and the experimental technique in Section 2, in Section 3 we describe the radiative recombination properties of localized and delocalized interwell excitons under conditions of resonant excitation by circularly polarized light when the pump power, electrical bias voltage, and temperature are varied. The time evolution of the spectra and the decay kinetics of the luminescence intensity of interwell excitons under conditions of pulsed laser excitation are discussed in Section 4. The diamagnetic properties of interwell excitons, their Zeeman splitting, and *g*-factor are presented in Section 5. In Section 6 we describe experiments using interwell excitons which accumulated in a lateral potential well of deformation origin far from the photoexcitation region. Finally in the concluding section 7 various properties of interwell excitons observed in their luminescence spectra and their critical behavior as a function of the optical pumping and temperature are interpreted in terms of collective exciton behavior.

2. EXPERIMENTAL TECHNIQUE AND STRUCTURES

We investigated GaAs/AlGaAs *n–i–n* heterostructures with a GaAs/AlAs/GaAs double quantum well and narrow AlAs tunnel barrier (4 ML) between the wells (the width of the GaAs quantum wells was approximately 120 Å and the AlAs barrier was approximately 11 Å). The entire structure was grown by molecular beam epitaxy on a (001)-oriented *n*-type doped GaAs substrate having an Si dopant concentration of 10^{18} cm^{-3}. First a 0.5 μm thick Si-doped (10^{18} cm^{-3}) GaAs buffer layer was grown on the substrate, followed by a 0.15 μm AlGaAs isolating layer ($x = 0.33$) and GaAs/AlAs/GaAs double quantum wells.

The heterojunction of each GaAs quantum well with the isolating AlGaAs layer was also separated by a narrow (4 ML) AlAs barrier. The narrow AlAs barriers were grown using a stop growth regime. In this growth technique the fluctuations of the AlAs barrier widths are large-scale. The double quantum wells were followed by a 0.15 μm thick isolating AlGaAs layer then a 0.1 μm thick Si-doped (10^{18} cm^{-3}) GaAs layer. Single broad GaAs quantum wells (of width ≈300 Å) were located in the isolating AlGaAs barriers near the doped regions. The luminescence from these quantum wells was used to assess the *e–h* excitations "percolating" toward the contact, doped regions of the structure and also to monitor qualitatively the density of interwell excitons building up in the double quantum wells under resonant excitation. The upper part of the structure was covered with a 100 Å thick GaAs layer. Mesas having dimensions of 1×1 mm were fabricated on the as-grown structure by a lithographic technique. Metal contacts of Au + Ge + Pt alloy were deposited as a frame on the upper part of the mesa and also the doped buffer layer.

The luminescence spectra were investigated under conditions of cw resonant excitation of intrawell direct heavy-hole excitons using a tunable Ti-sapphire laser. Circularly polarized resonant excitation was used to achieve optical orientation of the angular momentum in the exciton. The luminescence signal was analyzed using a circular analyzer. The time evolution of the luminescence spectra and their intensity kinetics were studied under pulsed excitation by a picosecond laser (wavelength 6200 Å, pulse duration 30 ps, repetition frequency 0.8 MHz). Pulsed measurements of the spectra and luminescence kinetics were made using a time-correlated photon counting system.

In order to detect the luminescence spectra we projected the optical excitation spot on the mesa onto crossed slits which were used to monitor the uniformity of the excitation and to select suitable regions of the structure for detection. Under cw excitation the luminescence spectra of the interwell excitons were also studied in the presence of a magnetic field perpendicular to the quantum-well planes (Faraday geometry). The diamagnetic shift of the excitons and their Zeeman splitting (σ^+, σ^- components of the spectra) were analyzed under these conditions.

3. LUMINESCENCE SPECTRA OF INTERWELL EXCITONS UNDER RESONANT PHOTOEXCITATION

In this section we shall analyze the behavior of the luminescence spectra of interwell excitons when intrawell spatially direct heavy-hole excitons (1*s*HH excitons) are resonantly excited by circularly polarized light. We are interested in how these spectra behave (their profile, intensity, and degree of circular polarization) when the excitation power density, applied electric field, and temperature vary.

3.1. Figure 1 shows luminescence spectra of intrawell (D) and interwell (I) excitons measured under resonant excitation and various applied electric fields. The optical transitions studied are illustrated schematically in Fig. 2. In the intrawell luminescence range at zero electric bias two lines can be identified, free, 1*s*HH, and bound excitons [15]. At low temperatures the direct exciton (line *D*) is observed as a weak "shoulder" on the violet wing of the exciton complex line. At negative electric fields from –0.3 V an interwell radiative recombination line appears which shifts almost linearly toward lower energies as the applied voltage increases in accor-

dance with the linear Stark shift of the size-quantization levels in the quantum wells (see inset to Fig. 1). Then only the line of the charged exciton complex remains significant in the intrawell recombination spectrum [15]. At higher negative fields $U < -0.4$ V under cw excitation only the photoluminescence line of the interwell excitons dominates in the spectra while the luminescence of the direct intrawell excitons and exciton complexes is of considerably lower intensity under these conditions.

The intensity of the interwell exciton line behaves nonmonotonically as a function of the applied bias. It appears in the luminescence spectrum at voltages when the Stark shift exceeds the difference between the binding energies of the intrawell and interwell excitons $eFz \geq E_D - E_I$.

At $U \sim -0.7$ V the intensity of this line has a maximum and then decreases with increasing electric field (see Fig. 1). This behavior is easily understood if we bear in mind that as the field increases, the effective dipole moment of the interwell exciton increases in the growth direction of the structure (z-axis) and the overlap of the electron and hole wave functions in the exciton decreases monotonically.

3.2. At fairly low temperatures (T = 2 K) and low pumping the luminescence line of the interwell excitons has a large width (FWHM = 4–5 meV) and the line profile itself is asymmetric with a fairly extended long-wavelength tail and relatively steep violet edge (see Figs. 1, 3). These characteristics of the photoluminescence line of the interwell excitons are a consequence of their strong localization at fluctuations of the random potential [6]. In this case the line width reflects the statistical distribution of the amplitudes of the random potential. The pumping levels are so low that the average density of the spatially separated electrons and holes is $n_{e-h} < 10^9$ cm^{-2}. At these concentrations the average statistical filling of lateral random potential wells having linear scales $l < 1$ μm by interwell excitons is less than unity and the inhomogeneous width of the photoluminescence spectrum of the interwell excitons is fairly large (Fig. 1).

The luminescence intensity, profile, and line width of the interwell excitons varies substantially as the power of the resonant excitation of direct intrawell excitons 1sHH by circularly polarized light increases (see Fig. 3). Line I narrows to 1.3 meV with increasing pumping, i.e., it becomes almost four times narrower. Its intensity at the maximum increases superlinearly while the line profile becomes almost symmetric or homogeneously broadened in contrast to the clearly inhomogeneously broadened profile of the photoluminescence spectrum of the interwell excitons at low excitation densities. In the strongly narrowing region the interwell exciton line is shifted by up to 1 meV toward lower energies as the pumping increases. Only at negligible pump powers $P > 6$ W/cm^2 does this line shift toward higher energies and become broader. A line shift toward higher energies indicates that the applied

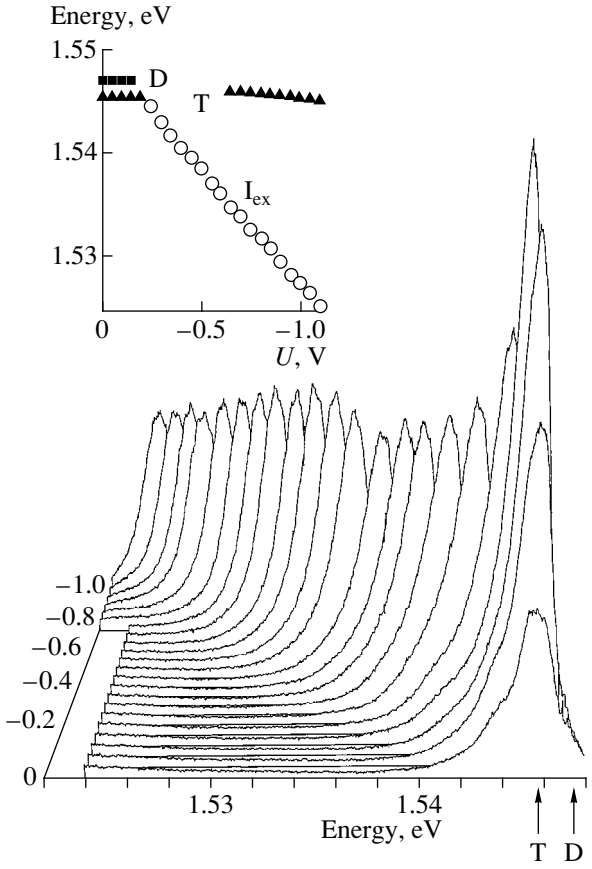

Fig. 1. Behavior of the luminescence spectra of interwell excitons as a function of applied voltage; T and D are the intrawell luminescence lines of an exciton complex and a direct 1sHH exciton at T = 2 K. The interwell exciton line (I) is constructed as a linear function of the applied electric field (see also inset to figure). The numbers to the left of the measured spectra correspond to the applied electric field. These photoluminescence spectra were measured at various applied voltages between 0 and –1.05 V at intervals of 0.05 V.

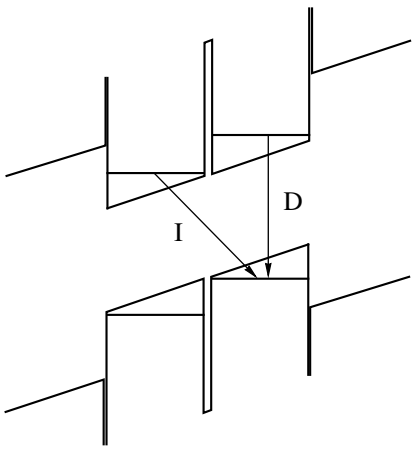

Fig. 2. Schematic of optical transitions on application of an electrical voltage which shifts the size-quantization levels in the double quantum wells. The arrows show the optical transitions corresponding to the intrawell (direct) D and interwell (spatially indirect) I excitons.

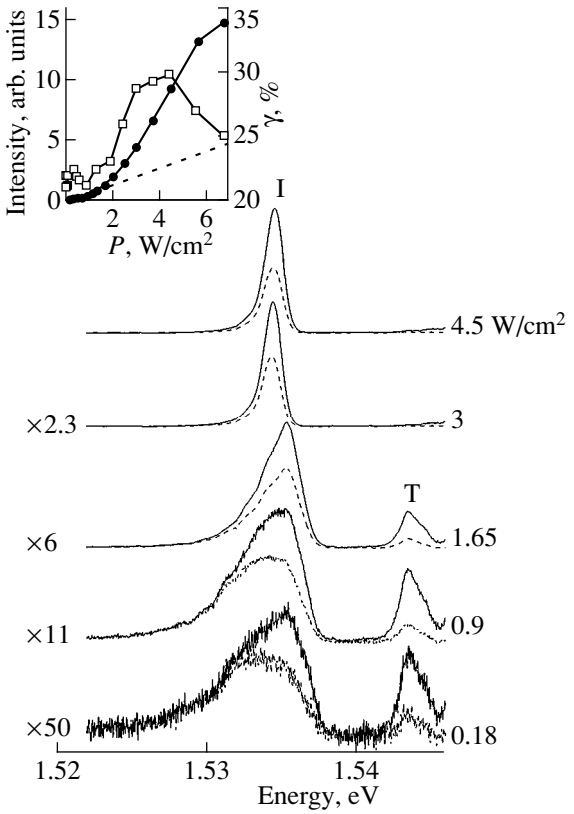

Fig. 3. Luminescence spectra and degree of circular polarization of interwell excitons for various optical pump powers under conditions of resonant excitation of heavy-hole intrawell excitons and $T = 1.8$ K: T and I are the lines of the intrawell exciton complex and an interwell exciton, the solid curves give the photoluminescence spectra measured for σ^+ polarization and the dashed curves give the spectra for the σ^- polarization. The numbers on the left of the spectra give the intensity scale factors and those on the right give the excitation power densities. The inset gives the photoluminescence intensity of line I (filled circles) and its degree of circular polarization (open squares) as a function of the power density. The dashed curve gives the linear approximation of the photoluminescence intensity of line I.

electric field is screened when the density of the interwell excitons becomes sufficiently high. Then, using the Gauss formula we can obtain an upper estimate of the interwell exciton density from the spectral shift. This estimate gives $n = 3 \times 10^{10}$ cm^{-2} for the concentration of interwell excitons when the line width becomes minimal. We observed appreciable narrowing of the luminescence line of the interwell excitons for various negative bias voltages between –0.5 V and –1.2 V. At high negative voltages similar narrowing of the interwell-exciton luminescence line occurred at significantly lower pump powers.

The strong narrowing of the interwell-exciton photoluminescence line at low temperatures suggests that at high excitation densities the lateral fluctuations of the random potential begin to be significantly screened. As a result of this screening of the random potential relief at fairly high pumping levels the interwell excitons lie above the percolation threshold (or the mobility threshold associated with the strong localization effect) and are delocalized. As the density of these delocalized interwell excitons increases, the narrow photoluminescence line is shifted toward lower energies (see Fig. 3). From this observation it follows that the ground-state energy of the interacting interwell excitons decreases as their density increases despite dipole–dipole repulsion. This behavior is typical of a dense system of Bose particles as their concentration increases at fairly low temperature.

3.3. The degree of circular polarization of the interwell-exciton luminescence line exhibits interesting behavior in the region where its intensity increases superlinearly with increasing resonant excitation power (see Fig. 3). In our experiments using circularly polarized exciting light, direct, completely spin-oriented 1*s*HH excitons were created for which the heavy-hole angular momentum is $J_h = +3/2$ and the electron spin $S_z = -1/2$. As a result of carrier tunneling and binding to form interwell excitons, and also as a result of spin–lattice relaxation and strong spin–orbit interaction for the holes, the spin "memory" of the interwell excitons is partially lost but still remains appreciable and is almost 5–10% at a low excitation density, although the interwell excitons are localized under these conditions and the corresponding photoluminescence line is inhomogeneously broadened. At constant pumping the degree of circular polarization of the interwell-exciton photoluminescence decreases monotonically with increasing bias voltage. As the power density of the resonant photoexcitation increases when the interwell-exciton photoluminescence line exhibits substantial narrowing, the degree of circular polarization of the corresponding line increases severalfold as a threshold process. Assuming that the rate of spin relaxation varies little with increasing pumping (most likely it only increases), this increase in the degree of circular polarization is naturally attributed to a reduction in the lifetime of the interwell excitons. This is deduced from a simple kinetic expression linking the degree of circular polarization with the lifetimes and spin relaxation [16]:

$$\gamma = \gamma_0/(1 + \tau_d/\tau_s),$$

where γ_0 and γ are the degrees of polarization of the intrawell and interwell excitons, and τ_d and τ_s are the radiative recombination and spin relaxation times of the interwell excitons, respectively. Assuming that τ_s is barely sensitive to the pumping, using this expression we can easily conclude that the experimentally observed trebling of the degree of circular polarization of the interwell excitons with increasing excitation power is a consequence of an at least fivefold increase in their rate of radiative annihilation. In the next section (Section 4) we discuss the lifetimes of interwell excitons determined directly using pulsed measurements.

3.4. When direct 1*s*HH excitons (polarized parallel to the layer plane) were excited resonantly by linearly

polarized light, as the pump power increased we observed a threshold increase in the linear polarization of the narrow photoluminescence line (alignment of interwell excitons) in the region of superlinearly increasing intensity. When the excitation densities were low and the interwell excitons were strongly localized at fluctuations of the random potential, their spectrum remained weakly polarized under the same conditions. The results of these experiments are illustrated in Fig. 4 which clearly shows an abrupt increase in the linear polarization of the interwell-exciton photoluminescence in a narrow range of pumping. This alignment of the lateral dipole moment of the interwell excitons reached a maximum and then decreased as the power density of the resonant excitation increased further, when screening of the applied electric voltage became appreciable (the pump range in which the photoluminescence line began to show appreciable broadening and shift toward higher energies).

3.5. Thus, as the concentration of interwell excitons increases, the intensity of the corresponding photoluminescence line increases superlinearly and the line exhibits strong narrowing while its degree of polarization increases, which indirectly indicates that the lifetime of the interwell excitons is reduced. These effects were very sensitive to temperature. We observed that when the temperature increased above critical values at high constant pump power, the line width of the interwell excitons increased abruptly and the degree of circular polarization dropped to its previous level. The temperature behavior of the degree of circular polarization and the photoluminescence line width of the interwell excitons are illustrated in Fig. 5. It can be seen that the critical temperature at which such dramatic spectral changes occurred in this case is $T_c \leq 6$ K ($\Delta T = \pm 1$ K).

4. KINETICS OF THE PHOTOLUMINESCENCE SPECTRA

In this section we shall discuss the time evolution of the luminescence spectra of intrawell and interwell excitons and also the kinetics of the intensities of the corresponding photoluminescence spectra under conditions of pulsed excitation using a picosecond laser.

Under these pulsed excitation conditions at the time of action of the laser pulse hot photoexcited electrons and holes are generated in each quantum well with equal density and not spatially separated. The spatial separation of the carriers between neighboring tunnel-coupled quantum wells is the result of complex kinetic processes involving intrawell relaxation and recombination of carriers and also carrier tunneling through the interwell barrier. Figure 6 shows the time evolution of the photoluminescence spectra under pulsed excitation measured for different delays relative to the exciting laser pulse at $T = 1.8$ K and applied voltage $U = -0.7$ V. For zero delays and integration of the signal with 1 ns time gates the spectra only reveal a region of direct intrawell luminescence. The photoluminescence spectrum of the interwell excitons only begins to form at

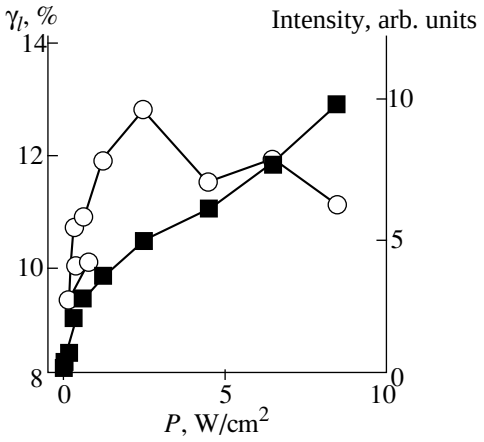

Fig. 4. Degree of linear polarization of interwell excitons (open circles) and photoluminescence intensity (filled squares) under resonant excitation of intrawell excitons by linearly polarized light as a function of optical pumping at $T = 1.5$ K.

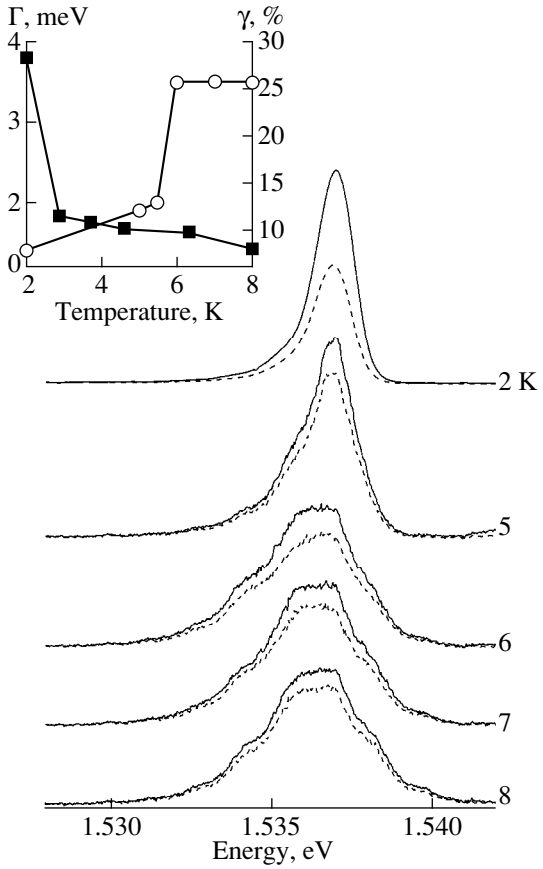

Fig. 5. Photoluminescence spectra of interwell excitons under resonant excitation by circularly polarized light, measured at various temperatures (numbers on the right of the spectra give the temperature) and optical pump power 3 W/cm^2. The solid curves give the photoluminescence spectra measured for the σ^+ polarization and the dashed curves give those for the σ^- polarization. The temperature dependences of the luminescence line width of the interwell excitons Γ and the degree of circular polarization γ are shown in the inset.

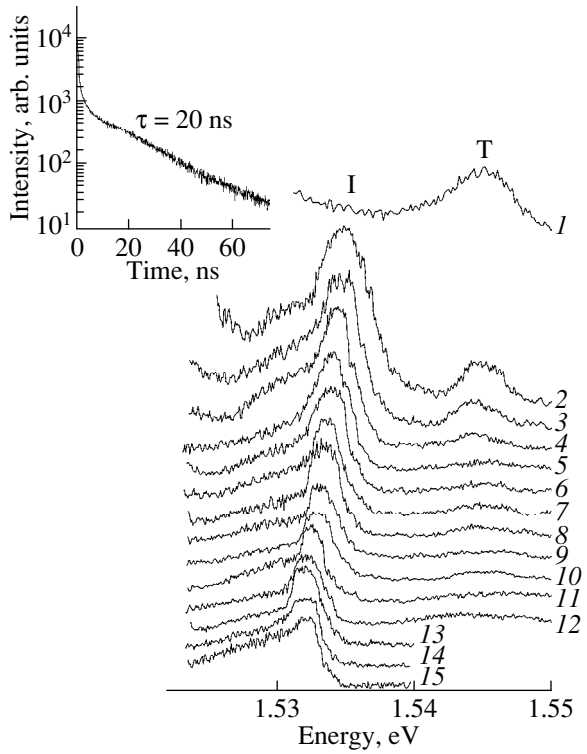

Fig. 6. Time evolution of the luminescence spectra of interwell excitons and intensity kinetics of the narrow line (see inset) under conditions of pulsed excitation and $T = 2$ K at –0.75 V. Spectrum *1* was measured with zero delay and an integration time of 1 ns; spectra *2–9* were measured with delays of 2, 3, 4, 5, 6, 7, 8, and 10 ns and an integration time of 2 ns; spectra *10–13* correspond to delays of 12, 16, 25, and 25 ns and integration times of 4, 4, 5, and 6 ns, respectively; spectra *14* and *15* correspond to delays of 30 and 40 ns and integration times of 10 and 12 ns, respectively.

time delays $\tau \geq 2$ ns. This delay is caused by carrier tunneling through the barrier (mainly electrons for which the effective mass in the vertical direction is much lower than the hole mass), accompanied by spatial separation of carriers between quantum wells, intrawell energy relaxation (thermalization) and simultaneous recombination. It can be seen from Fig. 6 that for small delays ($\tau = 2$–4 ns) the width of the interwell photoluminescence spectrum is large (3–4 meV). However, as the time delay increases, a fairly narrow line begins to form at the violet edge of the interwell photoluminescence spectrum. The width of this line is 1.5 meV for an 8 ns delay, i.e., the width is reduced almost threefold compared with that for the initial delays. The intensity of this line decays far more rapidly with time than the structureless interwell luminescence spectrum below it. For delays greater than 20 ns this line can no longer be resolved and merges with the structureless part of the spectrum whose profile remains almost unchanged and can be observed for delays greater than 50 ns. This behavior can be seen very clearly in the intensity kinetics measured directly at the spectral position of the narrow line and the structureless continuum below it (see inset to Fig. 6).

It is important to note that the narrow line of interwell-exciton photoluminescence characterized by short-lived intensity decay kinetics under pulsed excitation conditions is only observed at fairly low temperatures, as under cw excitation. For example, for a 12 ns delay the narrow line begins to become broader with increasing temperature and merges with the structureless background below it at $T \geq 6$ K. For shorter delays and therefore higher interwell exciton density this line disappears in the spectrum at significantly higher temperatures. For example, for a 7 ns delay the narrow line disappears in the spectra at $T \geq 9$ K. The interwell exciton lifetime can be measured directly from the intensity decay kinetics. In accordance with Fig. 6 (see inset), this time measured for a narrow photoluminescence line of delocalized interwell excitons at $T = 1.8$ K is 20 ns whereas the decay time of the broad photoluminescence band corresponding to localized exciton states is almost three times greater at 70 ns. This explains at least qualitatively why the degree of circular polarization of the narrow photoluminescence line of the delocalized excitons increases. Direct measurements of the intensity decay kinetics can be used to estimate the spin relaxation times in an interwell exciton. Using the formula given above for the degree of circular polarization and the measured lifetime of an interwell exciton at $T = 1.8$ K, we obtain for the spin relaxation time $\tau_s \sim 2 \times 10^{-8}$ s. The intensity decay kinetics of the narrow photoluminescence line are also sensitive to temperature and the corresponding decay time increases monotonically with decreasing temperature. For example, the decay time is $\tau = 20$ ns at $T = 1.8$ K whereas at $T = 5$ K we have $\tau = 10$ ns. The same qualitative behavior of the time-resolved spectra and the interwell photoluminescence kinetics was observed for applied voltages between –0.4 V and –0.9 V.

5. LUMINESCENCE SPECTRA OF INTERWELL EXCITONS IN A MAGNETIC FIELD

In this section we are interested in the diamagnetic properties of interwell excitons and their Zeeman splitting. These investigations were carried out at low excitation densities when the interwell excitons are strongly localized and their spectrum inhomogeneously broadened and at high pump densities when the photoluminescence line of the interwell recombination is substantially narrower. In these experiments we analyzed the Zeeman components σ^+ and σ^- of the interwell photoluminescence spectrum measured in a magnetic field perpendicular to the planes of the quantum wells (Faraday geometry).

Figure 7 shows the interwell photoluminescence spectra (σ^- component) measured when direct 1*s*HH excitons were resonantly excited at high power density in a magnetic field between 0 and 2 T at 0.1 T intervals.

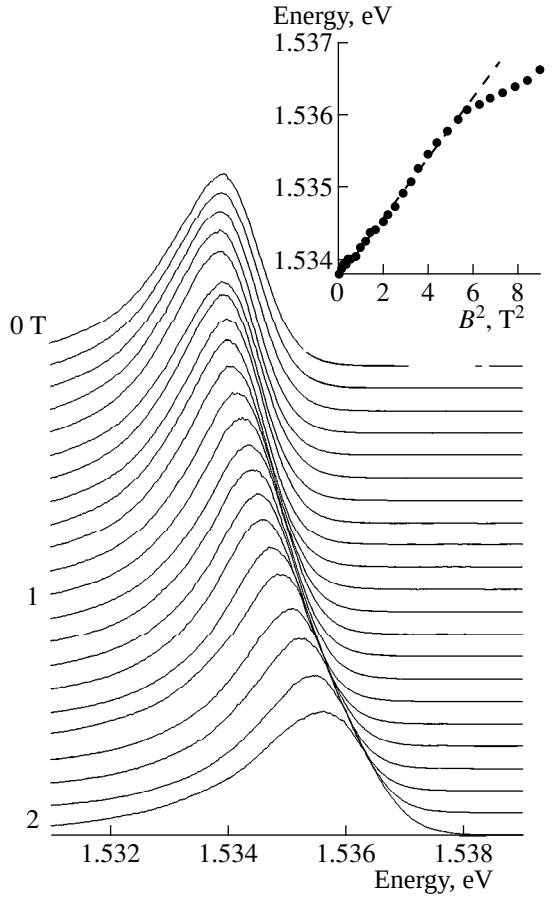

Fig. 7. Photoluminescence spectra of interwell excitons in a magnetic field perpendicular to the quantum-well plane and $T = 2$ K. These spectra were measured in the range 0–2 T at 0.1 T intervals. The spectra were measured using the σ^- polarization and pump power density 3 W/cm^2. The inset shows the diamagnetic shift of the delocalized interwell excitons.

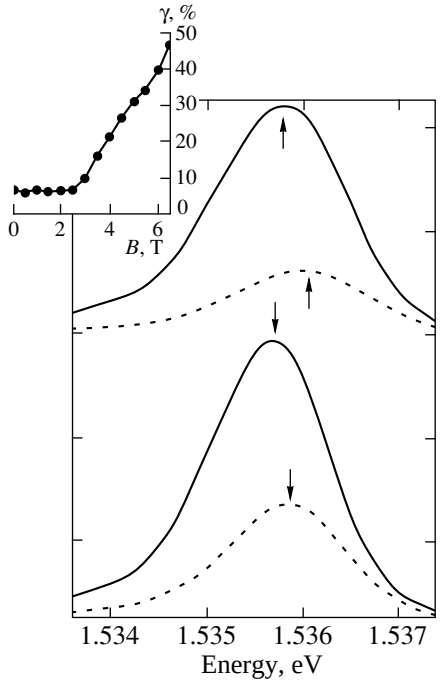

Fig. 8. Zeeman splitting of the photoluminescence line of delocalized interwell excitons at $B = 6.5$ T and $T = 2$ K. The solid and dashed curves correspond to the σ^- and σ^+ circular polarizations, respectively. The inset shows the intensity ratio of the Zeeman components as a function of the magnetic field.

The figure clearly shows a superlinear shift of the narrow photoluminescence line in the region of weak magnetic fields as B increases. The inset gives the spectral position of the maximum of the narrow interwell photoluminescence line as a function of the square of the magnetic field. The quadratic diamagnetic shift of this line is clearly satisfied in fields $B < 2$ T whereas in strong fields a linear contribution to the magnetic susceptibility begins to become significant [17]. Using a correction quadratic in B to the ground-state energy of an interwell exciton, we can estimate its Bohr radius in the quantum-well plane using the well-known formula:

$$\Delta E = \frac{e^2}{8\mu c^2} B^2 \langle a \rangle^2,$$

where $\langle a \rangle^2 = \pi a_B^2$ and μ is the reduced exciton mass ($m_e = 0.067 m_0$ and $m_h = 0.2 m_0$). The Bohr radius of an interwell exciton thus determined was $a_B = 170$ Å. From this we can obtain a lower estimate of the binding energy of an interwell exciton $E_{exc} = e^2/\epsilon a_B$ which was $E_{exc} \approx 3$ meV.

The narrow interwell-exciton line in a transverse magnetic field is split into a doublet, as in the case of an intrawell heavy-hole direct exciton. By way of example Fig. 8 shows the Zeeman splitting (σ^+ and σ^- components) of this line at $B = 6.5$ T. In this case unpolarized light was used for excitation (see lower part of Fig. 8). Figure 9 is a diagram of the allowed optical transitions predicted in Faraday geometry. The Zeeman splitting, which is 0.2 meV ($B = 6.5$ T) can be used to determine the effective g-factor of an interwell exciton $g_{exc} = 0.53$. The magnitude of the Zeeman splitting and the related effective exciton g-factor can also be determined using the intensity ratio of the corresponding σ^+ and σ^- components assuming that the spin states are uniformly populated and the electron temperature given. The independently determined exciton g-factor agreed to within 10% with the value obtained directly from the Zeeman splitting. We thus conclude that the distribution between the split spin states is quasi-equilibrium and also the temperature of the electron system is 0.2 K higher than the temperature of the helium bath at $T = 2$ K and pump power density 6 W/cm^2. Hence the optical pumping used experimentally does not strongly overheat the electron (exciton) system relative to the helium bath temperature and the lattice temperature.

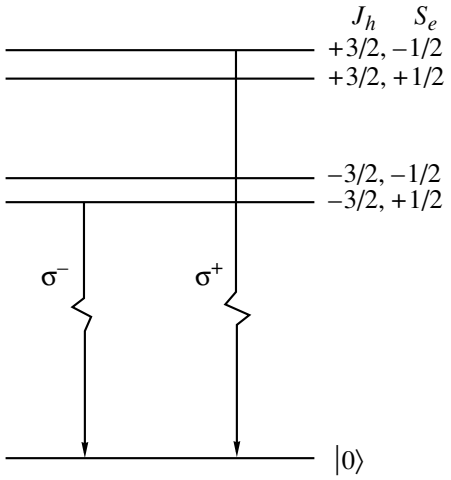

Fig. 9. Diagram of optical transitions under conditions of Zeeman splitting of the ground state of an interwell exciton.

The photoluminescence spectra shown in the upper part of Fig. 8 were measured under resonant excitation by circularly polarized light (σ^+ component). In this case, as can be seen from Fig. 8, the degree of circular polarization between the split Zeeman components increased more than 1.1 times compared with the photoluminescence spectra measured in the same magnetic field but excited by resonant unpolarized light. This experimental observation indicates that in a magnetic field under conditions of resonant photoexcitation by circularly polarized light the spin splitting in the exciton increases. In particular in a magnetic field B = 6.5 T this splitting increases 1.5 times and is 0.3 meV. The increase in the spin splitting in this case is naturally attributed to amplification of the effective electron g-factor:

$$\Delta E_{sp} = (|g_e^{\text{eff}}| + |g_h|)\mu_B B,$$

where the effective amplified electron g-factor is $g_e^{\text{eff}} = g_e^0 + (\Delta g)^{\text{eff}}$, and g_e^0 is the unperturbed ("bar") electron g-factor. The value thus determined in $(\Delta g)^{\text{eff}} = 0.27$ and the published value $g_e^0 = -0.44$. We attribute the amplification of the effective electron g-factor to alignment of the spins of the nuclear subsystem which occurs as a result of contact interaction between spin-oriented electrons excited by the circularly polarized light and nuclei of the dominant heterostructure material (in particular Ga nuclei, see for example [16]). In the presence of an external magnetic field this effect is significant since the field defines the preferential orientation of the nuclear spins. In the absence of an external magnetic field the orientations of the nuclear spins are random and the contributions of the various components compensate for each other.

We also investigated the photoluminescence spectra of interwell radiative recombination in a magnetic field at low excitation density when the interwell excitons are strongly localized at fluctuations of the random potential and the corresponding line in the spectrum is broad. In this case, the diamagnetic correction to the ground-state energy was determined from the dependence of the first moment M_1 of the photoluminescence spectrum of the interwell excitons on the square of the magnetic field ($M_1 = \int E\, I(E)dE / \int I(E)dE$). It was found that the diamagnetic correction to the energy for localized excitons is approximately 1.5 times this correction for delocalized excitons. The diamagnetic shift can be used to estimate the linear scales of lateral confinement associated with the random potential at which the interwell excitons are localized at low densities and low temperatures. This linear scale of localization was ~400 Å. The broad photoluminescence line of the localized interwell excitons in a magnetic field is also split into a Zeeman doublet. The doublet splitting and the exciton g-factor were estimated most accurately using the intensity ratio of the σ^+ and σ^- components. The value obtained for the g-factor was close to that for delocalized excitons.

6. BUILDUP OF INTERWELL EXCITONS IN A LATERAL POTENTIAL WELL FAR FROM THE PHOTOEXCITATION REGION

In previous sections we have discussed the spectra of interwell excitons measured under conditions where the luminescence was detected directly in the region of excitation on the mesa. In this section we discuss experiments in which interwell excitons accumulated in a lateral potential well far from the photoexcitation point. The interwell excitons were located in this potential well as a result of natural drift from the region of photoexcitation under the action of forces associated with the gradient of the strain potential. It was established that a potential well of strain origin appears in the quantum-well plane if a narrow (100 μm wide) metal (Au) stripe around 1 μ thick is deposited on the mesa surface of the structure. A substantial difference between the coefficients of thermal expansion of the metal stripe and the base material of the GaAs mesa gave rise to strain forces, which at liquid helium temperatures lead to nonuniform compression of the structure perpendicular to the quantum well plane. The largest strain occurred directly beneath the metal stripe and propagated inside the mesa. This strain was observed in particular in the fact that the luminescence line of the intrawell excitons measured directly beneath the metal stripe was spectrally shifted toward lower energies by around 1.5–2 meV as a result of mechanical compressive strain.

Experiments taking this into account were carried out as follows. An exciting laser spot smaller than 100 μm was focused near one of the sides of the metal stripe on the mesa surface. The mesa surface was projected onto the plane of crossed slits which could be used to monitor the "sampling" of the photoluminescence both directly from the region of excitation and at the opposite edge of the metal stripe, i.e., approximately 100 μ

from the exciting spot [regions (1) and (2) in Fig. 10 which shows the photoexcitation and detection conditions used experimentally]. These experiments were carried out using a GaAs/AlGaAs heterostructure (p–i–n structure) with a double quantum well (the width of the quantum well was 80 Å and the width of the AlGaAs barrier 40 Å). Figure 11 illustrates the behavior of the luminescence spectra at various pump powers when detected from region (2) some distance from the region of excitation. The luminescence from region (2) associated with interwell radiative recombination only became appreciable at high optical pump powers when the applied electric bias was strongly screened directly in the excitation zone (1) Thus, it can be seen from Fig. 11 that initially at low pump powers the interwell exciton line is strongly inhomogeneously broadened (its half-width is 4–5 meV) which is typical of low interwell exciton densities when these are localized at fluctuations of the random potential. With increasing pumping a narrow line begins to form at the violet edge of the photoluminescence spectrum. The intensity of this line increases superlinearly with increasing excitation power (see inset to Fig. 11) and the line itself narrows substantially, to a minimum width of 1.3 meV. The maximum of this narrow line is initially shifted toward lower energies (around 1–1.5 meV) and only at high pump powers does this line begin to broaden and shift into the violet as a result of screening of the applied electric field. This narrowing of the narrow photoluminescence line of the interwell excitons and superlinear increase in its intensity is observed when detected from region (2) at various applied bias voltages. Figure 12 illustrates the linear Stark shift of this line when the electric field is varied, which irrefutably indicates its interwell exciton nature. Direct measurements of the decay kinetics of the photoluminescence intensity made under pulsed excitation at various temperatures demonstrated (see Fig. 13) that the lifetime of delocalized interwell excitons at low temperatures, $T \leq 6$ K, i.e., when the corresponding photoluminescence line is narrow, is several times shorter than the lifetime of the localized interwell excitons (low pump powers or temperatures $T \geq 6$K).

These experiments have therefore demonstrated that the strong narrowing of the interwell radiative recombination line as the interwell exciton density increases is of a general nature in the presence of lateral confinement, either random (as a result of fluctuations of the random potential) or artificially created (accumulation of interwell excitons in a strain potential well far from the region of photoexcitation).

7. DISCUSSION OF EXPERIMENTAL RESULTS AND CONCLUSIONS

When we attempt to explain the complete set of experimental results presented above in terms of a simple single-particle picture of radiative annihilation of interwell excitons localized at fluctuations of the random potential, we encounter major difficulties. If the

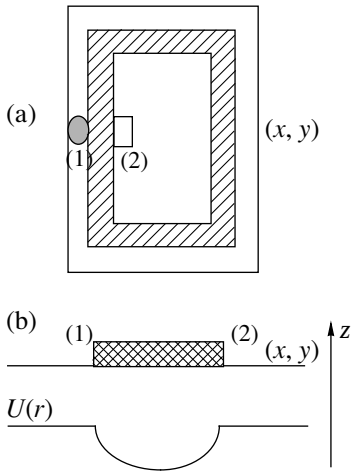

Fig. 10. Diagram of experiments to detect photoluminescence of interwell excitons far from the region of excitation. (a) Top view, metal stripe on mesa shown hatched, width of metal stripe 100 μm, (*1*) pump region, (*2*) region from which photoluminescence detected. (b) Qualitative picture of the deformation potential $U(r)$ beneath metal frame. The z direction is perpendicular to the quantum well plane (x, y).

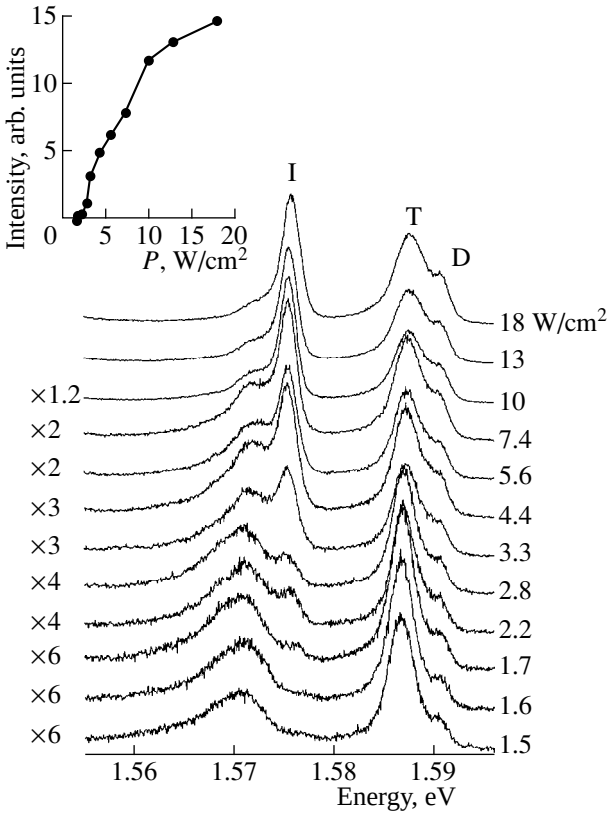

Fig. 11. Photoluminescence spectra of interwell I and intrawell D and T excitons at various pump powers, detected from region (2) on the mesa as shown in the experimental setup in Fig. 10. The numbers on the right of the spectra give the excitation power density and those on the left give the scale factors for the intensities of the corresponding spectra $T = 2$ K. The inset gives the intensity of the narrow interwell-exciton line as a function of the pump power density.

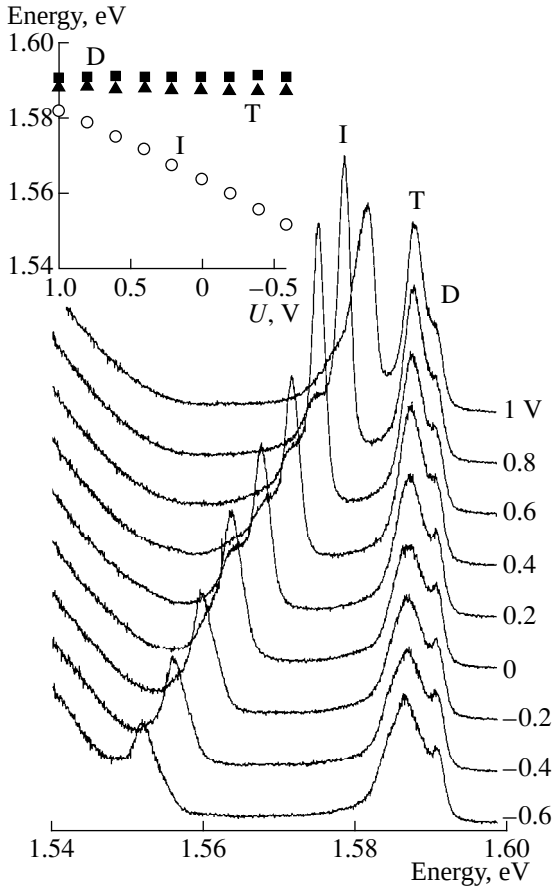

Fig. 12. Photoluminescence spectra of interwell excitons at various voltages: I, D, and T are the photoluminescence lines of the interwell excitons, direct intrawell excitons, and exciton charged complexes, respectively. The spectral position of the photoluminescence lines as a function of the electric field is illustrated in the inset top left.

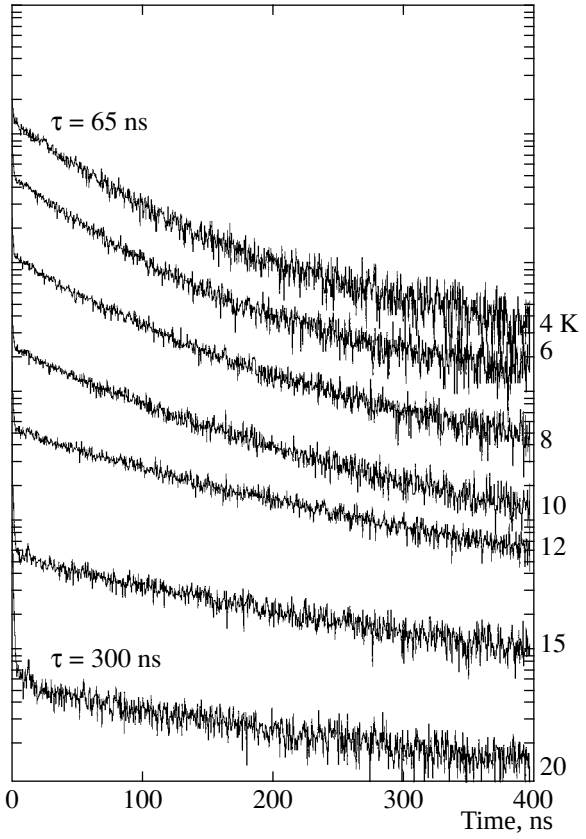

Fig. 13. Photoluminescence kinetics of the narrow interwell-exciton line at various temperatures (numbers on the right of the spectra).

appearance of a narrow line in the photoluminescence spectra is attributed to interwell delocalized excitons, which can appear above the percolation threshold as a result of screening of the random potential, it is difficult to explain why this effect is so temperature-critical and does not occur when $T > T_c$. The threshold increase in the degree of circular polarization and the alignment of the interwell excitons as their concentration increases are also completely unexplained. However, these results can be explained at least qualitatively as a consequence of the collective behavior of delocalized interwell excitons when a critical concentration and temperature are reached. It can be postulated these structures with narrow AlAs barriers exhibit large-scale fluctuations of the potential caused in particular by variations of the barrier width. These potential fluctuations are poorly screened, unlike the random potential, because of residual charge impurities which are also present in these structures. As a result of large-scale fluctuations of the potential relief in the quantum well plane photoexcited interwell excitons may accumulate in macroscopically extended regions with lateral confinement as far as several tenths of micron. In fact, variations of the effective lateral potential $U(r) = U(w(r))$ may be linked to variations of the quantum well width $w(r)$. Under quasiequilibrium conditions the lateral distribution of the exciton density will be determined by the equality $\mu(n(r)) + U(r) = \mu$, where μ is the chemical potential of the interwell excitons, which is related to their average density in the quantum wells, and $\mu(n)$ is the chemical potential of the homogeneous dielectric exciton phase in the lateral confinement region. Quite clearly $|\mu(r)| < |\mu|$ since $\mu(n) = -|E_{\text{exc}}| + |\delta U|$ (E_{exc} is the exciton binding energy) and the exciton density in the lateral confinement region may be substantially higher than the average density in the quantum well plane generated by the optical pumping. These are the regions where the main events associated with photoexcited interwell excitons take place. These events may evolve according to different scenarios but each is based on the assumption of collective interaction in a system of interwell excitons delocalized within macroscopically large lateral regions. In one scenario it could be postulated that on reaching critical densities and temperature the interwell excitons

condense to form a metallic *e–h* liquid with spatially separate electron–hole layers. If the narrow line in the spectrum is related to the metallic liquid phase, an upper estimate of its density can be obtained from the line width which, in this case, should be not less than the sum of the Fermi energies of the electrons and holes. Thus, the estimated density is 3×10^{10} cm^{-2} and the dimensionless parameter corresponding to this density is $r_s = 1/\sqrt{\pi n a_B^2} = 4$. Quite clearly the condensed phase in this approach is too "friable" to consider the Coulomb interaction in the interwell exciton completely screened. Hence at these concentrations excitons should retain their individuality so that the condensed phase cannot be metallic. This conclusion is also supported by studies of the photoluminescence spectra in a magnetic field in Faraday geometry. It was established (Section 5) that the narrow line, like a free exciton, splits into a Zeeman doublet with the intensity ratio of the σ^+ and σ^- components corresponding to the temperature and spin splitting, i.e., the individual properties of the exciton are completely conserved in the condensed phase.

We shall assume that strong narrowing of the interwell-exciton photoluminescence line and the sensitivity of this effect to density and temperature may be associated with the condensation of interwell excitons to form a collective dielectric exciton phase. It was shown in [14] that for specific values of the interwell-exciton dipole moment a fairly dense system of interwell excitons may condense to form a dielectric liquid despite the dipole–dipole repulsion between these excitons. It was also shown in [11] that when critical conditions are satisfied the collective phase of the interwell excitons is most likely to occur in regions with lateral confinement. According to our experiments using cw excitation such condensation occurs at $T < 5.5$ K and an average exciton concentration of 3×10^{10} cm^{-2}. Moreover, the narrowing of the photoluminescence line of the interwell excitons as their density increases at low temperature is accompanied by a systematic shift of this line toward lower energies (approximately by 1.5 meV). This behavior may be demonstrated by a fairly dense system of Bose quasiparticles having integer spin where $|\mu|/kT \longrightarrow 0$. However, the possibility of Bose–Einstein condensation of an exciton gas in systems of reduced dimensions is a very delicate and difficult problem [18]. Nevertheless, these observations serve as an independent argument in support of the assumption that in this particular case, we are dealing with a fairly dense dielectric collective phase in interwell excitons.

The condensed component of the excitons should be in phase within the coherence length. Spatial coherence should occur at least on scales of the de Broglie wavelength of an interwell exciton, λ_{ex} which at $T = 2$ K is $\lambda_{ex} = h/\sqrt{\pi m k T} = 1.5 \times 10^3$ Å and is more than an order of magnitude greater than the exciton Bohr radius ($a_B \sim 100$ Å). The exciton density under these conditions corresponds to the dimensionless parameter $r = n\lambda_{ex}^2 = 4$. Increased spatial coherence in the condensed phase is indicated by the observed threshold increase in the alignment of interwell excitons under conditions of resonant exciton by linearly polarized light. This alignment effect is directly related to the transverse relaxation and thus to the time of loss of phase coherence. A substantial increase in the alignment of interwell excitons which takes place as a threshold process may imply that the resultant collective exciton state has fairly long phase shift times (according to our estimates this time is around 1 ns at $T = 2$ K). Then the radiative decay of phase-correlated interwell excitons in the condensate should have significantly higher radiative probabilities compared with the photoluminescence of the uncondensed excitons. This conclusion also agrees with the experiment.

The assumption that interwell excitons condense to form a dielectric collective phase is nevertheless based on the unanswered important question concerning the spatial coherence scales of this collective state. This question may be answered using measurements of the photoluminescence intensity correlations under conditions when the postulated exciton condensation occurs.

ACKNOWLEDGMENTS

In conclusion, the authors thank S. Iordanskiĭ, A.S. Ioselevich, V.D. Kulakovskiĭ, R.E. Lozovik, V.G. Lysenko, and R.A. Suris for interesting discussions. This work was partly financed by the Russian Foundation for Basic Research (project no. 98-02-16656) and the Interdepartmental Program "Nanostructures."

REFERENCES

1. Yu. E. Lozovik and V. I. Yudson, Zh. Éksp. Teor. Fiz. **71**, 738 (1976) [Sov. Phys. JETP **44**, 389 (1976)].
2. T. Fukuzawa, E. E. Méndez, and J. M. Hong, Phys. Rev. Lett. **64**, 3066 (1990).
3. J. E. Golub, K. Kash, J. P. Harbison, and L. T. Flores, Phys. Rev. B **41**, 8564 (1990).
4. J. A. Kash, M. Zachau, E. E. Méndez, *et al.*, Phys. Rev. Lett. **66**, 2247 (1991).
5. L. V. Butov, A. Zrenner, G. A. Abstreiter, *et al.*, Phys. Rev. Lett. **73**, 304 (1994); L. V. Butov, in *Proceedings of the 23rd International Conference on Physics of Semiconductors, Berlin, 1996.*
6. V. B. Timofeev, A. I. Filin, A. V. Larionov, *et al.*, Europhys. Lett. **41**, 435 (1998).
7. V. B. Timofeev, A. V. Larionov, A. S. Ioselevich, *et al.*, Pis'ma Zh. Éksp. Teor. Fiz. **67**, 580 (1998) [JETP Lett. **67**, 613 (1998)].
8. V. V. Krivolapchuk, E. S. Moskalenko, A. L. Zhmodikov, *et al.*, Solid State Commun. **111**, 49 (1999).

9. D. Yoshioka and A. H. MacDonald, J. Phys. Soc. Jpn. **59**, 4211 (1990).
10. X. M. Chen and J. J. Quinn, Phys. Rev. Lett. **67**, 895 (1991).
11. Xuejun Zhu, P. B. Littlewood, M. S. Hybersten, and T. Rice, Phys. Rev. Lett. **74**, 1633 (1995).
12. J. Fernández-Rossier and C. Tejedor, Phys. Rev. Lett. **78**, 4809 (1997).
13. Lerwen Liu, L. Swierkowski, and D. Nelson, Physica B (Amsterdam) **249–251**, 594 (1998).
14. Yu. E. Lozovik and O. L. Berman, Zh. Éksp. Teor. Fiz. **111**, 1879 (1997) [JETP **84**, 1027 (1997)].
15. V. B. Timofeev, A. V. Larionov, M. Grassi Alessi, *et al.*, Phys. Rev. B **60**, 8897 (1999).
16. *Optical Orientation*, *Modern Problem in Condensed Matter Sciences*, Ed. by F. Mayer and B. Zhakharchenya (Elsevier, Amsterdam, 1984), Vol. 8.
17. G. E. W. Bauer and T. Ando, Phys. Rev. B **37**, 3130 (1988); **38**, 6015 (1988).
18. J. M. Kosterlitz and D. J. Thouless, J. Phys. C **6**, 181 (1973).

Translation was provided by AIP